

FATIGUE CHARACTERIZATION OF A HIGH-PERFORMANCE STEEL FIBER REINFORCED CONCRETE (HPFRC) BY MEANS OF COMPRESSIVE, FLEXURAL, AND Z-TYPE SHEAR TESTS

MARCO DAVOLIO^{1*}, HAMZA AHZAR¹, GIOVANNI VOLPATTI², ALFREDO A. FLOREZ GUTIERREZ³, DAVIDE ZAMPINI⁴, FRANCESCO LO MONTE¹ AND LIBERATO FERRARA¹

¹ Department of Civil and Environmental Engineering (DICA), Politecnico di Milano
P.zza Leonardo da Vinci 32, 20133 Milan, Italy
e-mail: marco.davolio@polimi.it, www.dica.polimi.it

² CEMEX Innovation Holding AG Brugg Branch
Römerstrasse 13, 2555 Brugg, Switzerland

³ CEMEX LATAM Holding AG Swiss Branch Brugg
Römerstrasse 13, 2555 Brugg, Switzerland

⁴ CEMEX Innovation Holding AG
General-Guisan-Strasse 6, 6300 Zug, Switzerland

Key words: Fiber Reinforced Concrete, Fatigue, Push-off

Abstract: The use of fiber-reinforced concretes (FRC) for infrastructures subject to fatigue loading can result into an extension of their service life by providing enhanced ductility and toughness. The cyclic actions might affect the fiber-matrix interface and it is necessary to assess to what extent the degradation hinders the mechanical properties of these materials. Currently, the only predictive models for fatigue life and performance reduction are empirical. Therefore, a mechanical characterization is required for any mix whose composition and performance might differ from the one pertinent to the database the models are based on. This work presents the effect of high-cycle fatigue on a high-performance fiber-reinforced concrete (HPFRC) with hybrid fiber reinforcement. The material was characterized under compressive, flexural, and shear loads at various stress ranges. The Palmgren-Miner rule was applied to predict the fatigue life of the material. The results showed the effects of fatigue loading on the strength of the material. The compressive strength remained constant in most cases, while the flexural and the shear performances were slightly reduced by the cycling process. The predictive capacity of the P-M model proved to be reliable only in limited scenarios.

1 INTRODUCTION

The growing demand for strategic infrastructures raised the attention towards the development of durable materials. Structures like highway pavements, bridge decks, and wind turbines are subject to millions of

loading cycles during their service life [1]. The repeated variation of the stress state degrades the material, affecting its mechanical properties and, eventually, can lead to the failure of the structural element [2]. Hence, fatigue life prediction plays a crucial role for

the design of the aforesaid types of structures.

The fundamental degradation mechanism related to fatigue is the formation of an initial damage in the concrete matrix and its propagation along the applied cyclic load path [3]. Fiber-reinforced concrete (FRC) features a remarkable toughness compared to plain concrete [4]. When a crack forms, concrete is no longer able to transfer the stress between the two fracture surfaces. Thus, the fibers activate and provide a bridging effect, ensuring the continuity of stress transfer. As a matter of fact, in ordinary reinforced concrete (ORC) the cracking process is controlled only through reinforcement bars, which are located at a given distance from the surface. Therefore, the initial damage can freely propagate until it reaches the reinforcement. Conversely, for fiber-reinforced concrete the bridging effect acts at the early stage of the cracking process since the fibers are homogeneously distributed inside the matrix. For a given loading condition a specific crack opening is expected. Hence, design codes report the requirements to limit the crack opening under the fundamental combinations of actions. While fatigue cycles might range between two given loading conditions and, hence, stress levels, the damage progressively increases. This phenomenon is related to multiple factors. As described by Zhang et al. [5], the fatigue loading degradation is due to the microscopic changes at the aggregate-paste and fiber-matrix interfaces, as well as the fiber rupture due to abrasion.

Currently, the studies available in literature involving fatigue loading of FRC mainly investigated the flexural response [5,6]. As a matter of fact, for compressed elements the fibers play a limited role since they activate after cracking, which is less likely to happen under the compression stress levels allowed in design limit states. On the other hand, the residual capacity of a compressed FRC member after fatigue cycles might be hindered by the repetitive variation of the stress state. Furthermore, in terms of compressive strength the increase provided by high-performance concrete (HPC) already proved to enhance fatigue resistance [7,8]. Thus, an experimental

characterization which involves both the compressive and the tensile behavior of the material is required.

From a structural perspective, the design codes approach the fatigue degradation of ORC structures by means of empirical models [9]. The models provide the expected service life and the performance reduction as functions of the number of cycles and the stress state for each cycle. One of the most common predictive models for fatigue life estimation is the Palmgren-Miner (P-M) rule. This model is based on a linear accumulation of damage (1). The damage D is defined as the sum of the ratios between the applied cycles n at a given stress level i - and the total number of cycles to failure N for the same stress level.

$$D = \sum_i \frac{n_i}{N_i} \quad (1)$$

The P-M model was introduced for fatigue effects on steel elements and then adopted for concrete structures. In ORC structures steel reinforcement controls the damage propagation at macroscale and, thus, the model might be reliable. For FRC structures the proposed models might need to be adapted since fibers act at smaller scale and they are homogeneously distributed inside the concrete matrix.

The present work proposes the mechanical characterization of a high-performance fiber-reinforced concrete (HPFRC) under fatigue loading. Different stress states, number of cycles and stress levels were investigated, as detailed in Section 2. The results are presented and discussed in Section 3 in terms of performance degradation. Section 4 provides a critical application of the Palmgren-Miner rule to the experiments performed and an alternative approach based on the accumulation of damage.

2 EXPERIMENTAL PROGRAMME

The experimental campaign reported in this paper has investigated the mechanical properties of a tailored high-performance fiber-reinforced concrete (HPFRC), commercially known as Cemex® Resilia®. The mix design is protected under the Patent

EP3307692 B1 [10].

The experimental campaign included three different stress states: compression, bending, and shear. A total of 30 specimens was produced for each case. The geometry of the specimens is reported in Table 1.

Table 1: Geometry of the specimens

Test	Specimen	Geometry [mm]
Compression	Cylinder	220×110 (h×d)
Bending	Prism	600×150×150 (l×b×w)
Shear	Cube	150×150×150 (l×l×l)

Six monotonic tests were conducted to characterize the properties of the material under static loading for each loading state (Figure 1).

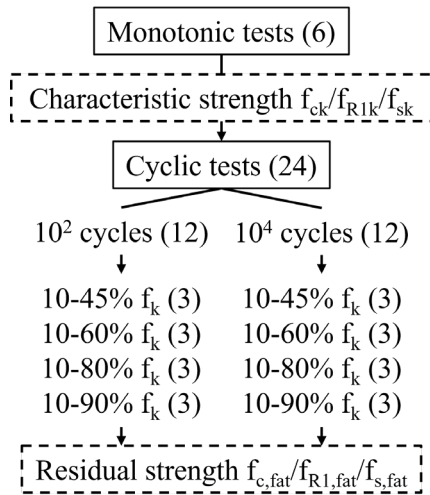


Figure 1: Scheme of the experiments.

Three samples were tested for each case of fatigue loading. The loading conditions for the cyclic tests were defined according to the results of the monotonic tests. A frequency of 3 Hz was adopted to simulate the service conditions of numerous infrastructures. The cycles were executed under load control, applied as a sinusoidal wave. Four stress states were investigated, with the same lower boundary, equal to 10% of the relative characteristic static strength, and an upper boundary respectively equal to 45%, 60%, 80%, and 90% of the same static characteristic

strength values. Two different total numbers of cycles were applied: 10^2 and 10^4 . For cyclic tests, the procedure included four steps: (a) loading up to the mid-point, (b) cyclic test, (c) unloading, and (d) failure test. No initial damage was induced in the specimens.

The compressive tests were performed according to the EN 12390-3 Standard. For the flexural characterization, three-point bending tests were performed according to the EN 14651 Standard. Since there are no standards currently available for direct shear tests of FRC, a tailored testing layout was developed, as shown in Figure 2. The geometry represented was defined as “Z-type push-off” and is characterized by a cube with two horizontal notches with 35 mm net spacing in between. By compressing the cube, the central section is subject to a quasi-pure shear stress state. A visual inspection during and after the tests confirmed that the failure mode was coherent with the expected crack pattern related to a pure shear stress state (Figure 2).

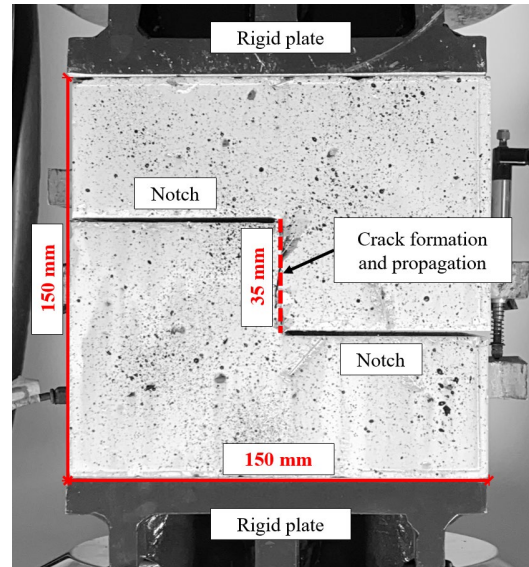


Figure 2: Layout of the Z-type push-off test.

3 RESULTS

3.1 Compressive tests

The performance under compression was evaluated in terms of residual peak strength after the fatigue test. The evolution of the average value over cycles is shown in Figure 3. Compressive strength is mainly related to

the performance of the matrix, while fibers only provide ductility at the cracked stage [11]. The latter only appears after reaching the peak strength. Hence, the results are less affected by the fibers content and distribution inside the specimen.

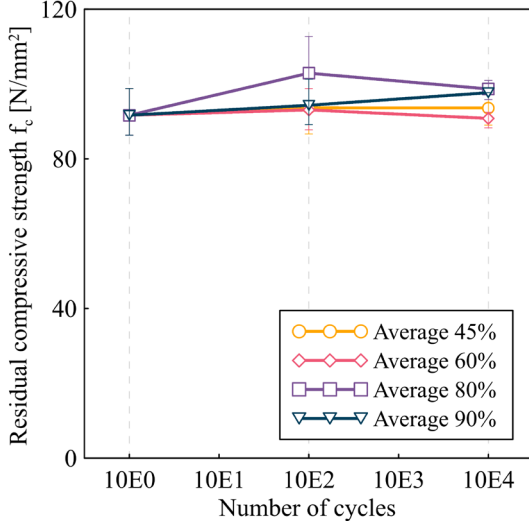


Figure 3: Residual compressive strength f_c after cycles.

The graphs show the capacity of the material to maintain its compressive strength after the cycles. Since fibers are not involved until after reaching the maximum strength of the material, the material did not experience any performance reduction. These results confirmed what already observed by Guo et al. [12], with similar fatigue life for the stress levels of 0.6, 0.8, and 0.9.

3.2 Flexural tests

Standard flexural tests results are expressed in terms of residual strengths f_{Rj} ($j = 1, 2, 3, 4$). Each parameter is associated with a given crack mouth opening displacement (CMOD). The most relevant parameters are f_{R1} and f_{R3} – CMOD of 0.5 mm and 2.5 mm respectively – since they are used for the structural design and material performance classification as well [9,13]. The evaluation of the residual strength for flexural tests raises an open question. Unlike compression and shear, for which the main parameter is the peak strength, the flexural strength is defined by given levels of CMOD. The accumulation of damage due to fatigue shifts the failure curve from the origin

to the residual crack opening (Figure 4). Therefore, the residual strength parameters can be obtained either neglecting or considering the residual CMOD (Δ_{CMOD}). The former case is pertinent to the structural design, since it evaluates the same condition analyzed during the design phase. Conversely, operating a shift on the curve before the evaluation of the residual flexural strengths might be suitable for the characterization of the material. As a matter of fact, the shape of the post-fatigue curve matches the monotonic tests, as already observed by Carlesso et al. [14]. Therefore, any apparent performance loss related to the accumulated CMOD and not to an actual decrease of strength can be more truly assessed by shifting the curve. The difference between the two values is directly proportional to the damage accumulated during the test. The graph in Figure 5 shows the evolution of the error (2) with respect to the accumulated CMOD. f_{Rj} represents the residual resistance at fixed CMOD values (i.e., 0.5 mm and 2.5 mm), while f_{Rj}' includes the shift of the experimental curve to the origin. A higher scattering can be observed for f_{R1} values, which are in the first branch of the curve.

$$e = \frac{f_{Rj} - f_{Rj}'}{f_{Rj}} \quad (2)$$

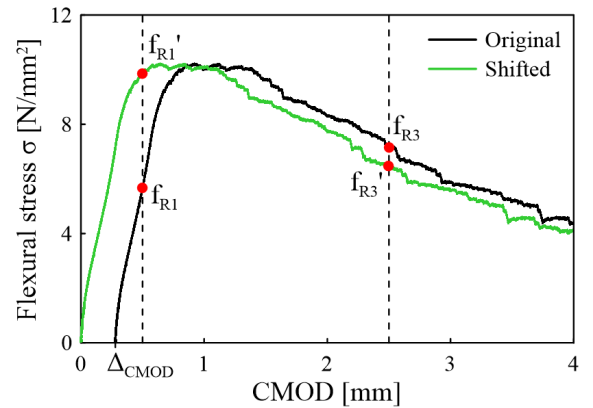


Figure 4: Bending curves with and without shifting.

Given the above observations, the evolution of the residual flexural strength over cycles was evaluated in terms of f_{R3} only. The selected parameter is less affected by the scattering related to the calculation method

and is referred to the ultimate limit state for structural design. The graph in Figure 6 shows the values of f_{R3} for the static cases and after the cyclic tests. The application of cyclic loads on the beams reduced the ductility of the element, which exhibited a decreasing trend in most cases. These results find good agreement with the ones obtained by Monteiro et al. [15], which described the degradation of the fiber-matrix interface due to fatigue. The accumulated damage weakens the bond between the fibers and the surrounding paste, reducing the bridging capacity of the reinforcement and, thus, the ductility of the element. The difference between the two number of cycles is not significant enough to observe further degradation. The range of values obtained can be attributed to the variable number of fibers on the critical specimen cross section, a governing factor for FRC elements subject to tensile regimes [16,17].

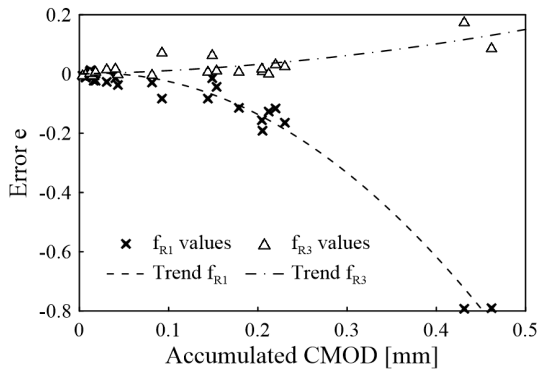


Figure 5: Trend of the error with respect to the damage.

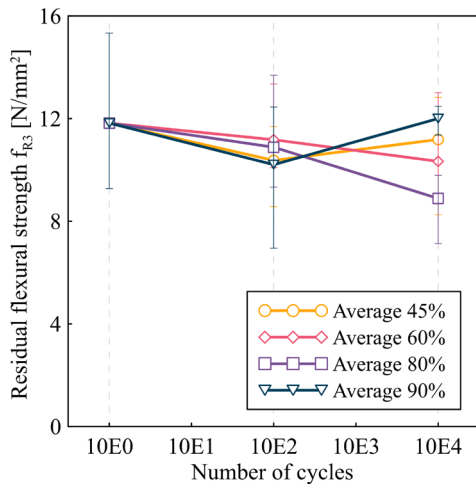


Figure 6: Residual flexural strength f_{R3} after cycles.

3.3 Z-type shear tests

The results of push-off tests exhibited some scattering due to the geometry of the specimen. The layout introduced permitted a quasi-pure shear stress state in the central section of the samples to be obtained. However, the number of fibers crossing the section is strictly dependent on the casting process and has a remarkable effect on the strength [18].

The graph in Figure 7 shows the effect of higher stresses applied during the fatigue load path on the residual shear strength. For the specimens cycled between 10% and 45% of the characteristic strength, the damage induced by fatigue did not affect the performance of the material. The slightly increasing trend can be reasonably attributed to the variable fiber content across the ligament cross-section.

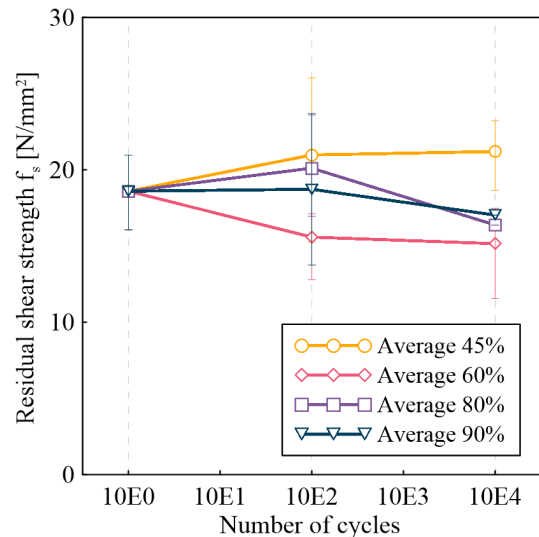


Figure 7: Residual shear strength f_s after cycles.

The higher stress levels investigated resulted in a progressive decrease of the residual strength after cycles. In these cases, the crack in the central section of the specimen formed during the cycling process. For this reason, the reduction in the performance could be a consequence of the more significant degradation occurring at the fiber-matrix interface during cycles, for increasing upper stress levels, as already described by Zhang et al. [5].

4 FATIGUE FAILURE

4.1 The Palmgren-Miner predictive model

The Palmgren-Miner (P-M) model is the formulation provided by the fib Model Code [9] to predict the fatigue damage for a given stress range. The residual capacity can be both defined in terms of strength and number of cycles. Hence, it is possible to predict the expected number of cycles to failure N minimizing the difference between the two terms (3) (4).

$$\frac{d}{dN} \sqrt{\sum_i \left[\left(1 - \frac{n_i}{N}\right) - \frac{f_{fat,i}}{f} \right]^2} = 0 \quad (3)$$

$$N = \frac{\sum_i n_i^2}{\sum_i n_i \times \left(1 - f_{fat,i}/f\right)} \quad (4)$$

where n_i is the number of cycles experienced by the i -sample, $f_{fat,i}$ its residual strength after cycles, and f is the characteristic static strength of the material. The equation applies to any loading condition.

The P-M model was applied to the experiments performed to critically evaluate its predictive capability and effectiveness. Firstly, the model works only if the experimental results show a degrading trend. In some cases, an apparent increase in the performance was observed because of the scattering. Thus, the predictive model was not applied. Moreover, when the degradation is not significant – for residual performances of 90-95% – the model might provide an underestimation of the cycles to failure, due to the logarithmic shape of the curve.

Figure 8 summarizes all the possible predictions obtained with the P-M model. Compressive tests exhibited an almost constant performance in terms of residual strength. Therefore, the model was able to predict failure at approximately 10^6 cycles for the 10-60% stress level, remarkably higher than the number of cycles applied during the experiments. Moreover, when the upper boundary of the cycles was 90% two specimens failed prematurely and, thus, the expected fatigue life is close to 10^4 cycles. A

similar behavior was observed for shear tests, for which the degradation at 10-60% range was already visible after 10^2 cycles, but the additional cycles did not further reduce the performance. Hence, the curve predicts a service life close to 10^5 cycles, while for the highest stress level the degradation progressively reduced the residual performance at each step, resulting in a predicted service life close to 10^4 cycles.

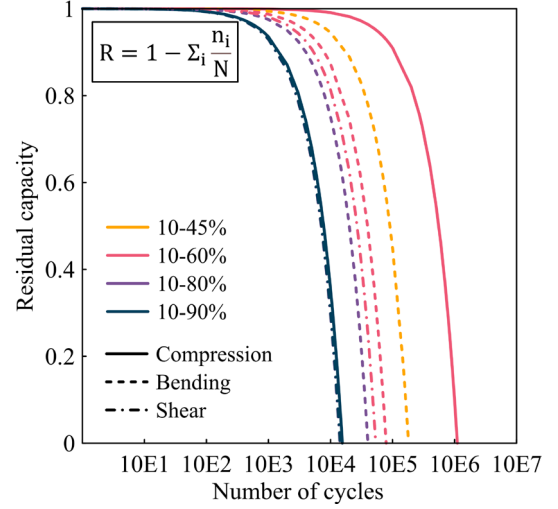


Figure 8: Prediction of fatigue life with the P-M model.

The fatigue life under cyclic flexural loading could be predicted in three different load ranges. A reduction of the service life was observed with the increasing upper stress boundary. In all cases the predicted number of cycles to failure exceeded the cycles applied on the specimens. Thus, the model was in good agreement with the experimental observations, since no premature failure was observed during the tests. Despite the effectiveness of the predictions provided by the P-M model in this work, few studies already discussed the tendency to under- or over-estimate the actual fatigue life of fiber-reinforced concrete [19,20]. For this reason, enhanced models might be applied to the experimental results obtained and compared to the standard P-M formulation. An important concern regarding the Palmgren-Miner model is its dependance on the experimental results populating the predictive equation. When premature failure is not observed, the

prediction obtained with the P-M model might not be appropriate to represent the fatigue resistance of the investigated material. For this reason, two bending tests were conducted up to 10^6 cycles to evaluate the accuracy of the model itself. Since both tests, with 10-45% and 10-60% stress levels respectively, did not experience premature failure, the P-M prediction was adjusted with the additional values of residual strength. As shown in Figure 9, the effect of the two additional experimental points is significantly pushing the expected cycles to failure of the material, thus meaning that any material must be tested up to failure to have an appropriate estimation of its fatigue resilience.

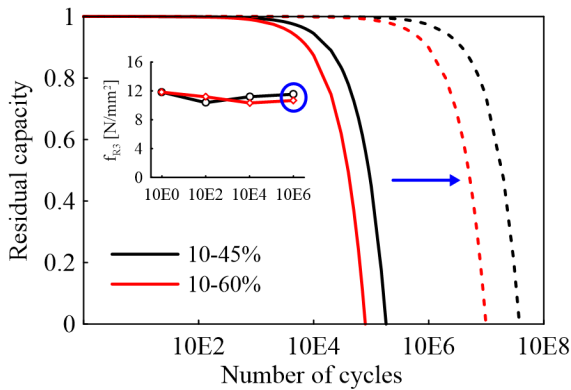


Figure 9: Effect of the experimental values on the P-M model predictive capacity.

4.2 Unstable crack growth

Stephen and Gettu [21] proposed an alternative approach to determine the damage pattern that leads to fatigue failure. As discussed above, fatigue is strictly related to the damage experienced by the structural element during cycles. The progression of damage can be monitored with specific sensors. Thus, any change of the damage progression pattern can be identified. When the deterioration of the element exceeds a given threshold, the progression becomes unstable. A sudden increase in the damage accumulation happens subsequently and leads to the failure. Stephen and Gettu introduced the concept of critical crack opening, defined as the threshold of the unstable propagation. The onset of the unstable condition could be

observed only for the specimens that failed prematurely. Due to the limited number of cycles applied, the failure was achieved in only few cases. Premature failure happened for two specimens tested under compression and five specimens tested under shear.

The graph in Figure 10 shows the evolution of the damage for a shear test conducted at 10-80% stress levels. For this type of test, the damage is the displacement associated to the crack opening in the central section and the subsequent relative slip of the two parts of the specimen. The material was able to withstand the progression of the cycles accumulating a limited damage up to about 1400 cycles. After reaching a threshold of 0.4 mm, the additional damage at each cycle started to increase exponentially up to the failure, which happened at 1486 cycles. For all the premature failures, the damage accumulated before the onset of the unstable displacement growth was approximately 0.15 mm with respect to the initial damage due to pre-loading.

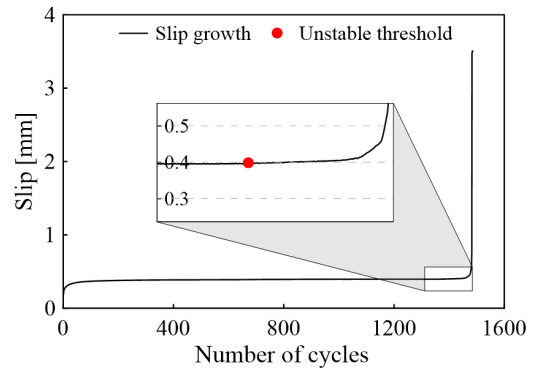


Figure 10: Evolution of the damage and onset of the unstable condition over cycles.

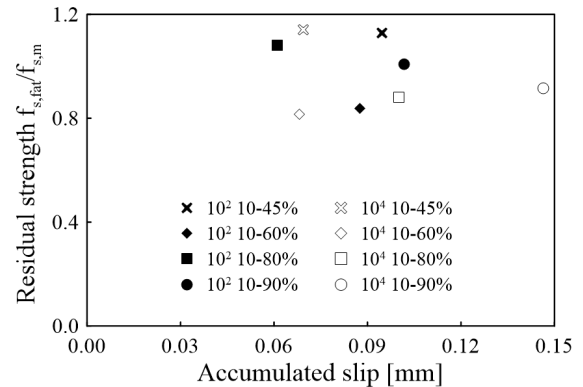


Figure 11: Accumulated slip and residual strength of the push-off tests.

The results discussed above can be related to the push-off tests that did not experience the premature failure. As shown in Figure 11, all the specimens accumulated less displacement than the unstable threshold, identified as 0.15 mm.

Given the correlation discussed above, it is possible to extend the same approach to the other tests conducted. The specimens tested under 3-point bending always completed the prescribed number of cycles, even the ones at higher stress levels. However, it is possible to correlate the damage accumulated – evaluated in terms of CMOD – with the residual strength of the material after cycles. As already described in Section 3.2, the parameter adopted for the residual strength is f_{R3} . The graph in Figure 12 shows the variation of the ratio between the residual strength after cycles and the average value of the monotonic tests with respect to the CMOD accumulated during the cycles.

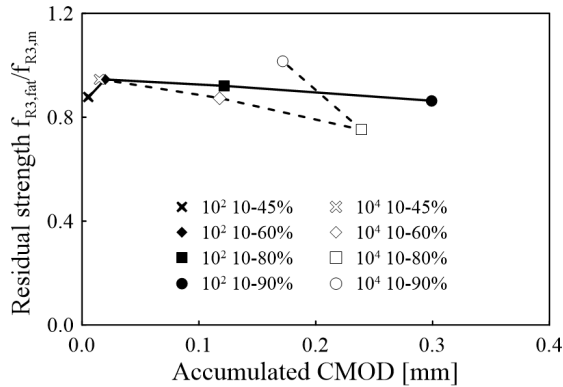


Figure 12: Accumulated CMOD and residual flexural strength f_{R3} .

Two main observations can be drawn from the experimental results. Firstly, the damage accumulated is directly proportional to the upper boundary of the stress levels applied during the fatigue tests and to the number of cycles. The value related to 10^4 cycles at 10-90% stress level can be considered an outlier, as already discussed in Section 3.2. An increased number of cycles is associated with a higher accumulation of CMOD due to the progressive degradation of the fiber-matrix interface and the slip of the fibers inside the concrete matrix. Moreover, both the results at

10^2 and 10^4 cycles show a decreasing residual strength when a more significant damage is accumulated during the fatigue test. Hence, a further progression of the damage might be associated with the failure of the specimen due to fatigue, as observed for the push-off tests. In the case of 3-point bending, the critical threshold was never reached and, thus, it was not possible to identify it. As a matter of fact, the works available in the literature show that a higher number of cycles is required to achieve failure during the cyclic loading regime [5,22].

The specimens tested under compression did not experience significant degradation in terms of performance. Hence, for this type of tests the correlation between the damage – expressed as accumulated strain – and the residual strength was not as straightforward as for the flexural tests. However, the graph in Figure 13 confirms that the damage accumulated during cycles is directly proportional to the stress levels applied and to the number of cycles.

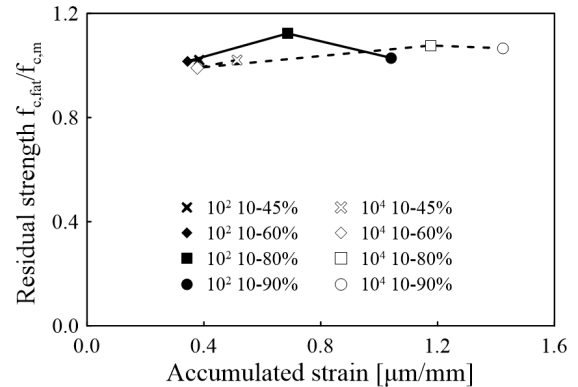


Figure 13: Accumulated strain and residual compressive strength f_c .

The effect of the former is more significant at higher stress levels, while the difference between 45% and 60% is negligible. The two curves have a similar trend, but the one associated with 10^4 cycles shows higher absolute values of accumulated damage.

5 CONCLUSIONS

This work has investigated the effects of high-cycle (10^2 and 10^4) fatigue loading on a high-performance fiber-reinforced concrete

with hybrid fiber systems. Different loading regimes, number of cycles and stress levels were tested.

The compressive strength remained constant in most cases owing to the presence of various fibers acting at different scales to prevent significant damage accumulation under fatigue.

The effect of cyclic loading on the flexural performance was observed in terms of residual strength f_{R3} , indicating a loss of toughness due to the deterioration of the fiber-matrix interface during the test.

The Z-type push-off testing layout was able to induce a quasi-pure shear failure mode on the critical cross section of the specimen. The effects of fatigue were comparable to the flexural response, as both loading regimes strongly affect the bond between the fibers and the surrounding cement paste, reducing the crack-bridging effect at failure.

The Palmgren-Miner rule could reasonably predict the fatigue life in most cases. However, an enhanced formulation might be more appropriate for HPFRC materials to determine their service life under cyclic actions as well as the need to complement the present experimental campaign with tests at even higher number of cycles (10^6) to provide a more wide and solid database for the application of the rule.

The present work proved the efficiency of high-performance fiber-reinforced concretes for infrastructures subject to fatigue loading during their service life, which, after the applied cyclic load-paths, did not experience any significant loss of performance, as far as the investigated cases are concerned.

An alternative approach based on the accumulation of damage was also investigated. The effectiveness of the method was proved from multiple perspectives. Firstly, it was possible to determine a critical damage accumulation threshold for the Z-type push-off tests. Moreover, the damage accumulated during the flexural tests could be related to the performance degradation after cycles. A clear trend that correlates the accumulated CMOD with the residual strength reduction could be identified. However, the accumulation of

damage proved to be less effective for the compressive tests, since the performance reduction related to fatigue was negligible in most cases.

Acknowledgements

Dr. Giuseppe Pappadà, Mr. Paolo Broglia, Arch. Maria Santangelo, Mr. Francesco Pillai, M.Sc. Giacomo Vazzana, and Mr. Marco Antico, technicians from the Laboratory of Testing Materials (LPM) of Politecnico di Milano are kindly acknowledged for their technical support during the experiments.

REFERENCES

- [1] Kachkouch, F.Z., Noberto, C.C., de Albuquerque Lima Babadopulos, L.F., Melo, A.R.S., Machado, A.M.L., Sebaibi, N., Boukhelf, F., and El Mendili, Y., 2022. Fatigue behavior of concrete: A literature review on the main relevant parameters. *Constr. Build. Mater.* **338**:1-22.
- [2] Wang, C.S., Zhai, M.S., Duan, L. and Wang, Q., 2015. Fatigue service life evaluation of existing steel and concrete bridges. *Adv. Steel Constr.* **11**:305-321.
- [3] Lee, M.K. and Barr, B.I.G., 2004. An overview of the fatigue behaviour of plain and fibre reinforced concrete. *Cem. Concr. Compos.* **26**:299-305.
- [4] Otter, D.E. and Naaman, A.E., 1988. Properties of Steel Fiber Reinforced Concrete under Cyclic Loading. *ACI Mater. J.* **85**:254-261.
- [5] Zhang, J., Stang, H. and Li, V.C., 1999. Fatigue life prediction of fiber reinforced concrete under flexural load. *Int. J. Fatigue* **21**:1033-1049.
- [6] Banjara, N.K. and Ramanjaneyulu, K., 2018. Experimental Investigations and Numerical Simulations on the Flexural Fatigue Behavior of Plain and Fiber-Reinforced Concrete. *J. Mat. Civ. Eng.*

- 30**:1-15.
- [7] Lohaus, L., Oneschkow, N., Elsmeier, K. and Hümme, J., 2012. Fatigue behaviour of high performance concretes for wind turbines. *Bautechnik* **89**:533-541.
- [8] Nguyen, D.-L., Thai, D.-K. and Lam, M.N.-T., 2022. Synergy in Flexure of High-Performance Fiber-Reinforced Concrete with Hybrid Steel Fibers. *J. Mat. Civ. Eng.* **34**:1-16.
- [9] Fédération internationale du béton (fib), 2010. *fib Model Code for Concrete Structures 2010*.
- [10] Esser, J., Guerini, A., Volpatti, G. and Zampini, D., 2019. Advanced fiber reinforced concrete mix designs and admixture systems. *Patent EP3307692 B1 [priority 2015-06-11]. Commercially available as Cemex® Resilia®*.
- [11] Lee, S.C., Oh, J.H. and Cho, J.Y., 2015. Compressive behavior of fiber-reinforced concrete with end-hooked steel fibers. *Materials* **8**:1442-1458.
- [12] Guo, M., Feng, Z. and Chen, Y., 2017. Research on material fatigue test of steel fiber reinforced concrete under tension and compression loading. *Key Eng. Mater.* **730**:353-357.
- [13] di Prisco, M., Plizzari, G. and Vandewalle, L., 2009. Fibre reinforced concrete: new design perspectives. *Materials and Structures* **42**:1261-1281.
- [14] Carlesso, D.M., Cavalaro, S. and de la Fuente, A., 2021. Flexural fatigue of pre-cracked plastic fibre reinforced concrete: Experimental study and numerical modeling. *Cem. Concr. Comp.* **115**:1-11.
- [15] Moreira de Alencar Monteiro, V., Taissum Cardoso, D.C. and de Andrade Silva, F., 2023. Mechanisms of fiber-matrix interface degradation under fatigue loading in steel FRC. *J. Build. Eng.* **68**:1-14.
- [16] Kang, S.T., Lee, B.Y., Kim, J.K. and Kim, Y.Y., 2011. The effect of fibre distribution characteristics on the flexural strength of steel fibre-reinforced ultra high strength concrete. *Constr. Build. Mater.* **25**:2450-2457.
- [17] Herrmann, H., Boris, R., Goidyk, O. and Braunbrück, A., 2019. Variation of bending strength of fiber reinforced concrete beams due to fiber distribution and orientation and analysis of microstructure. *IOP Conf. Ser.: Mater. Sci. Eng.* **660**:1-12.
- [18] Zhao, Y., Bi, J., Wang, Z., Huo, L., Guan, J., Zhao, Y. and Sun, Y., 2021. Numerical simulation of the casting process of steel fiber reinforced self-compacting concrete: Influence of material and casting parameters on fiber orientation and distribution. *Constr. Build. Mater.* **312**:1-23.
- [19] Murthy, R.A., Aravindan, M. and Ganesh, P., 2018. Prediction of flexural behaviour of RC beams strengthened with ultra high performance fiber reinforced concrete. *Struc. Eng. and Mech.* **65**:315-325.
- [20] Baktheer, A., Hegger, J. and Chudoba, R., 2019. Enhanced assessment rule for concrete fatigue under compression considering the nonlinear effect of loading sequence. *Int. J. Fatigue* **126**:130-142.
- [21] Stephen, S.J. and Gettu, R., 2020. Fatigue fracture of fibre reinforced concrete in flexure. *Materials and Structures* **56**:1-11.
- [22] Chen, D. and El-Hacha, R., 2011. Behaviour of hybrid FRP-UHPC beams in flexure under fatigue loading. *Compos. Struct.* **94**:253-266.